Improving Accuracy of Pseudo Zernike Moments using Image Interpolation

Chandan Singh
Professor, Department of Computer Science
Punjabi University
Patiala-147002, Punjab, India

Rahul Upneja
Research Fellow, Department of Computer Science
Punjabi University
Patiala-147002, Punjab, India

ABSTRACT

Pseudo Zernike Moments (*PZMs*) are very popular moments among the family of orthogonal radial moments. While several methods have been proposed to enhance accuracy, accurate *PZMs* computation for gray level images is still an open issue. *PZMs* suffer from image discretization error, geometric error and numerical integration error, which result in the degradation of the reconstructed images for high order of moments. It is observed that these errors are significant for the small images. In this paper, *PZMs* are computed after image interpolation on the small size images. Bi-cubic interpolation is used to increase the number of sampling points of the image. Experimental results show that the proposed method provides much improved accuracy of *PZMs* which provide very accurate reconstructed images, numerical stability and rotation invariance.

General Terms

Digital Image Processing, Pseudo Zernike Moments.

Keywords

Pseudo Zernike moments, Geometric error, Numerical integration error, Bi-cubic interpolation, Recursive method.

1. INTRODUCTION

Zernike Moments (*ZMs*) and Pseudo Zernike Moments (*PZMs*) are most popular moments among the family of circularly orthogonal moments. They have been used in optical character recognition, pattern classification, face recognition, content based image retrieval, image watermarking, image reconstruction etc.[1-8]. *PZMs* are observed to be superior than *ZMs* in terms of their feature representation capabilities, since pseudo-Zernike polynomials contain $(p_{max}+1)^2$ linearly independent polynomials of order $\le p_{max}$, whereas Zernike polynomials contain only $(p_{max}+1)(p_{max}+2)/2$ linearly independent polynomials due to the condition $p-q=even$. *PZMs* are less sensitive to image noise than the *ZMs* [9,10]. Apart from being rotation invariant, they can be made scaling and translation invariant after certain geometric transformations [11,12].

The conventional direct method which depends on zeroth order approximation produces geometric error and numerical integration error in *PZMs* calculation. By inscribing the circle inside square image, the information loss occurs due to the inexact approximation of the circular boundary of the image [13]. To overcome the geometric error, Wee and Paramesran

[14] proposed an alternative mapping technique in which the complete image is contained inside the unit disk. Therefore, all pixels are involved in the computation of radial moments. However, this enhances the domain of calculation. The second source of error is from sampling the kernel functions of moments at pixel center, which is referred to as the numerical integration error. However, the higher number of sampling points of an image gives better approximation and reduces numerical integration error. The higher order moments which are mainly affected by numerical integration error, are required for better representation of an image and for its accurate reconstruction. The image discretization error, geometric error and numerical integration error are more pronounced in small images. Therefore, applications such as optical character recognition and template matching in which small images are used, are more prone to these errors when *PZMs* are used as features. Numerical instability is another problem which is observed in moment calculation. Numerical instability occurs when the images are small and moment orders are high. The traditional zeroth order approximation of *PZMs* calculation makes *PZMs* numerically unstable for moment order $p_{max}>20$. There are, however, fast recursive algorithms [15] which make them stable even for moment orders upto 40 for an image of size 32×32 pixels.

The geometric error and numerical integration error are reduced if the resolution of the image is increased. It is shown by Liao and Pawlak [13] that the geometric error is of the order $O(N^{-15/22})$, where N is the resolution of a square image in one direction. The numerical integration error is reduced if the kernel function of *PZMs* is sampled at more number of points instead of a single point on a square grid. The increased resolution of an image is obtained by image interpolation from a lower resolution image. There are various interpolation techniques in the literature for image interpolation but the performance of bi-cubic interpolation [16,17] is found to be most appropriate when a good tradeoff between accuracy and speed of calculation is required.

In this paper, we propose bi-cubic interpolation technique to reduce the image discretization error for representing a discrete image function by a piecewise continuous function. The resulting continuous image function is then used to compute the *PZMs* at higher resolutions which, in turn, reduce the geometric error and numerical integration error thus providing very accurate *PZMs*. Numerical stability is achieved by resorting to recursive relations for the fast computation of *PZMs*. The enhanced accuracy of *PZMs* results in better image reconstruction and improved invariance to rotation.

2. PSEUDO ZERNIKE MOMENTS

2.1 Basic Formulation

The *PZMs* of order p and repetition q of a two dimensional image function $f(r,\theta)$ over a unit disk are defined by

$$A_{pq} = \frac{p+1}{\pi} \int_0^{2\pi} \int_0^1 f(r,\theta) V_{pq}^*(r,\theta) r dr d\theta \qquad (1)$$

where the image function $f(r,\theta)$ is defined over discrete square domain $N \times N$ and $V_{pq}^*(r,\theta)$ are the complex conjugate of the pseudo Zernike polynomials $V_{pq}(r,\theta)$, given by

$$V_{pq}(r,\theta) = R_{pq}(r) e^{jq\theta} \qquad (2)$$

where p is a non-negative integer, $0 \leq |q| \leq p, j = \sqrt{-1}$, $r = \sqrt{x^2 + y^2}, \theta = \tan^{-1}\left(\frac{y}{x}\right)$.

A_{pq} is often split into real and imaginary parts, A_{pq}^R and A_{pq}^I, as given below

$$A_{pq}^R = \frac{p+1}{\pi} \int_0^{2\pi} \int_0^1 f(r,\theta) R_{pq}(r) \cos(q\theta) r dr d\theta \qquad (3)$$

$$A_{pq}^I = -\frac{p+1}{\pi} \int_0^{2\pi} \int_0^1 f(r,\theta) R_{pq}(r) \sin(q\theta) r dr d\theta \qquad (4)$$

The radial polynomials $R_{pq}(r)$ are expressed as

$$R_{pq}(r) = \sum_{s=0}^{p-|q|} (-1)^s \frac{(2p+1-s)! r^{p-s}}{s!(p+|q|+1-s)!(p-|q|-s)!} \qquad (5)$$

Since the integration in Eq.(1) does not have an analytical solution, it is approximated in a discrete domain as [13]

$$A_{pq} = \frac{p+1}{\pi} \sum_{\substack{i=0 \\ x_i^2 + y_k^2 \leq 1}}^{N-1} \sum_{k=0}^{N-1} f(x_i, y_k) V_{pq}^*(x_i, y_k) \Delta x_i \Delta y_k \quad (6)$$

where (x_i, y_k) is the centre of the pixel (i,k) given by

$$x_i = \frac{2i+1-N}{D}, \; y_k = \frac{2k+1-N}{D}, \; i, k = 0, 1, ..., \; N-1 \, (7)$$

and

$$\Delta x_i = \Delta y_k = \frac{2}{D} \qquad (8)$$

The pixel (i,k) has an elemental area $\Delta x_i \Delta y_k$ which represents the grid $[a_i, b_k] \times [a_{i+1}, b_{k+1}]$ where,

$$a_i = \frac{2i-N}{D}, \; b_k = \frac{2k-N}{D}, \; i, k = 0, 1, ..., \; N$$
$$(9)$$

$$D = \begin{cases} N & \textit{for inscribed circular disc contained} \\ & \quad \textit{in the square image} \\ N\sqrt{2} & \textit{for outer circular disc containing} \\ & \quad \textit{the whole square image} \end{cases}$$

Figure 1(a) represents an 8×8 image. Figure 1(b) is an inscribed circular region of the image where the circular boundary is approximated by square grids for which $x_i^2 + y_k^2 \leq 1$. For this circle, $D = N$. Figure 1(c) describes the outer circle which encloses the square image completely and for which $D = N\sqrt{2}$.

In the first mapping process, given in Fig. 1(b), the pixels whose centers fall outside the boundary of the unit disk are ignored. The centers of many square grids on image boundary lie outside the circle and, therefore, these square grids are left out in the process of moment calculation. On the other hand, a square grid whose center lies inside the circle takes part in the calculation even though a part of it falls outside the circle. This creates geometric error in the computation of moments. However second approach given in Fig. 1(c) removes geometric error but increases the domain of computation. We use both mapping approaches to observe the results for the proposed algorithm.

Suppose that moments of all orders and repetitions $\leq p_{\max}$ are given, then the image is reconstructed as follows.

$$\hat{f}(x_i, y_k) = \sum_{p=0}^{p_{\max}} \sum_{q=-p}^{p} A_{pq} V_{pq}(x_i, y_k), i, k = 0, 1, ..., \; N-1 \qquad (10)$$

The closeness of reconstructed image function $\hat{f}(x, y)$ with the original image function $f(x, y)$ reflects the ability of a method to describe an image. The fidelity criterion which measures this closeness is expressed in terms of mean square reconstruction error (*MSRE*) represented by ε and defined by

$$\varepsilon = \frac{\sum_{i=0}^{N-1} \sum_{k=0}^{N-1} \left(f(x_i, y_k) - \hat{f}(x_i, y_k) \right)^2}{\sum_{i=0}^{N-1} \sum_{k=0}^{N-1} f^2(x_i, y_k)} \qquad (11)$$
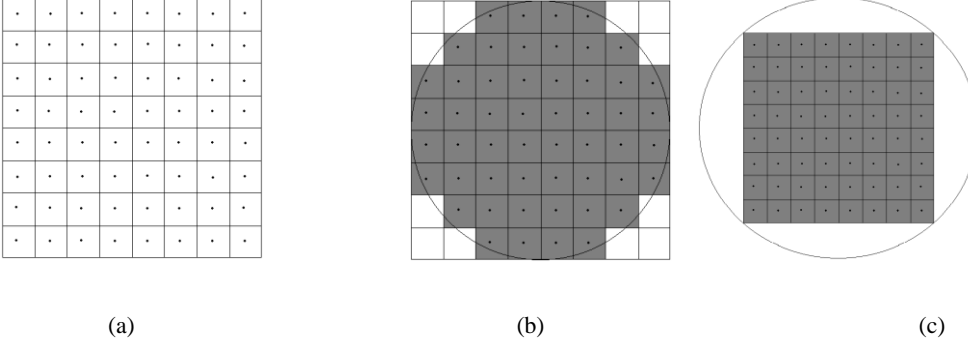
Fig.1: (a) An 8×8 image, (b) inscribed circle approximated by square grids, (c) outer circle containing the whole square image.

2.2 Recurrence Relation for $R_{pq}(r)$

It can be observed that the computation of radial polynomial $R_{pq}(r)$ is time consuming. In order to enhance the speed there are many approaches, among them the recursive methods [15] are found to be very useful and numerically stable. The recursive methods are characterized by reduced time complexity. A *p*-recursive method for the calculation of radial polynomials of *PZMs* is given by [15].

$$R_{qq}(r) = r^q \qquad (12)$$

$$R_{(q+1)q}(r) = (2q+3) r^{q+1} - 2(q+1) r^q \qquad (13)$$

$$R_{pq}(r) = (k_1 r + k_2) R_{(p-1)q}(r) + k_3 R_{(p-2)q}(r),$$
$$p = q+2, q+3, ..., p_{\max} \quad (14)$$

where

$$k_1 = \frac{2p(2p+1)}{(p+q+1)(p-q)},$$

$$k_2 = -2p + \frac{(p+q)(p-q-1)}{(2p-1)} k_1$$

$$k_3 = (2p-1)(p-1) - \frac{(p+q-1)(p-q-2)}{2} k_1 + 2(p-1)k_2 \quad (15)$$

3. THE PROPOSED ALGORITHM

The zeroth order approximation of the *PZMs* defined by Eq.(1) is given by Eq.(6). We resample the image function using interpolation for better approximation of the image function. Bi-cubic interpolation [16] is used to resample the image function, which uses sixteen 4×4 neighboring pixels for its estimation. The bi-cubic interpolation given by Keys [16] is commonly used for digital images. It has been proved by Reichenbach and Geng [17] that other advanced methods provide marginal improvements in interpolation at the cost of a high complexity of computation and their implementation. Let $(x, y) \in [a_i, b_k] \times [a_{i+1}, b_{k+1}]$, then the function value $f(x, y)$ within the grid is represented by

$$f(x,y) = \sum_{l=-1}^{2} \sum_{m=-1}^{2} f(a_{i+l}, b_{k+m}) u\left(\frac{x - a_{i+l}}{h_x}\right) u\left(\frac{y - a_{k+m}}{h_y}\right) \quad (16)$$

where u is the interpolation kernel as given below and h_x and h_y are the x and y coordinates sampling increments.

$$u(s) = \begin{cases} \frac{3}{2}|s|^3 - \frac{5}{2}|s|^2 + 1, & 0 < |s| < 1 \\ -\frac{1}{2}|s|^3 + \frac{5}{2}|s|^2 - 4|s| + 2, & 1 < |s| < 2 \\ 0, & 2 < |s| \end{cases} \quad (17)$$

The interpolation on the image boundaries are treated as special cases. For more details, one can refer [16]. For experimental purpose, we resample the image by taking 4×4 sampling points within each grid for maintaining a balance between speed and accuracy. However, higher sampling points give better approximation of an image but it takes much more time for computation. After performing the bi-cubic interpolation over an image, we perform zeroth order approximation as given in Eq.(6) for the computation of *PZMs*. We use recursive algorithms for the computation of radial polynomials which not only reduce the time complexity, but also provide numerical stability.

4. EXPERIMENTAL ANALYSIS

The computational framework presented in this paper is implemented in Visual C++6.0 under Windows environment on a PC with 3.0 GHz CPU and 3GB RAM. We take twelve standard gray scale images which are normally used for various image processing analysis [14]. The original images are 256×256 pixels in size which are resized to 64×64 pixels.

4.1. Accuracy and Reconstruction Capability

The experiments are performed for the three cases: (i) & (ii) the zeroth order approximation using the direct approach, and recursive approach, respectively, and (iii) the proposed approach using bi-cubic interpolation of image. The results are presented both for the inscribed circle, i.e., $D = N$ and outer circle, i.e., $D = N\sqrt{2}$.

The average *MSRE* for twelve images with respect to the order of moment is depicted in Fig.2 and Fig.3 for inscribe circle and for outer circle, respectively. For the proposed method, *MSRE* decreases with respect to the increase in p_{max}. It is shown that the *MSRE* is much lower by using the proposed method for high order of moments for both inscribed circle and outer circle.
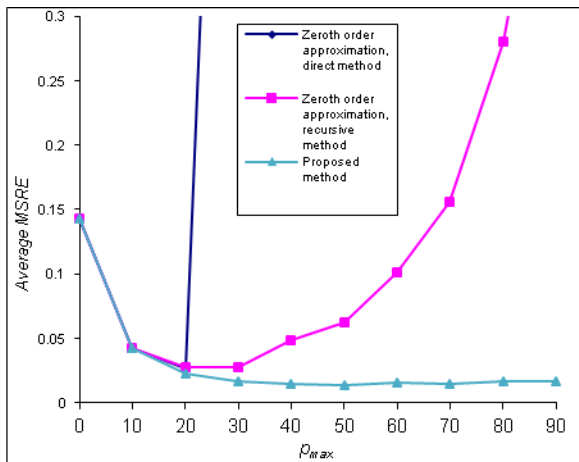
Fig.2: Average mean square reconstruction error, ε , as a function of order of moments for twelve standard images of 64×64 pixels (inscribed circle).
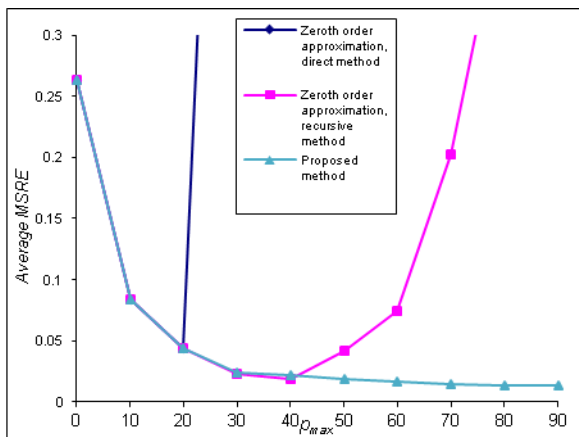
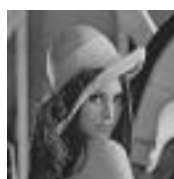**Fig.3: Average mean square reconstruction error, ε , as a function of order of moments for twelve standard images of 64×64 pixels (outer circle).**

Fig.4: Lena 64×64 image (one of the standard images of size 256×256 pixels which is resized to 64×64 pixels).

It may be recalled that the *MSRE* represents the gross aspect of image reconstruction error, it does not provide the local trend of instability in *PZMs*. This is clear in figures which illustrates the visual aspects of reconstructed images using *PZMs*. The experiments are conducted on 64×64 Lena image which has high contrast of gray values. Figure 4 displays the original Lena image and Fig. 5 and Fig.6 represent the reconstructed images using various methods and different moment orders p_{max}. The quality of the reconstructed images shows that the zeroth order approximation using direct method of the computation of *PZMs* is highly unstable and it is observed that for $p_{\max} > 20$ the magnitude of *PZMs* assume high values. However, the images reconstructed using

recursive method are numerical stable except in the vicinity of the centre of the circle. The instability is reflected through white spots around the centre and it increases with the increase of the moment order p_{max}. On the other hand, the quality of reconstructed images using proposed method is far better than that of traditional methods. There is no white spot in the vicinity of the centre of the circle, both for inscribed circlular disk and outer circle. The proposed method using bi-cubic interpolation have better reconstruction capability and numerical stablity as compared to traditional methods.

p_{max} \ methods	Zeroth order approximation direct method	Zeroth order approximation recursive method	Proposed method
10	ε=0.042737	ε=0.042737	ε=0.042002
20	ε=0.027620	ε=0.027772	ε=0.023173
30	ε=very high	ε=0.027477	ε=0.016936
40		ε=0.048682	ε=0.015022
50		ε=0.062792	ε=0.014192
60		ε=0.101469	ε=0.01536
70		ε=0.155714	ε=0.014933
80		ε=0.28176	ε=0.017029

Fig.5: Reconstructed image of Lena 64×64 using *PZMs*, with different orders, $p_{\max} = 10 \; to \; 80$ for inscribed circle.
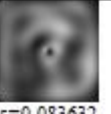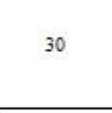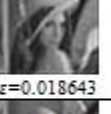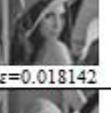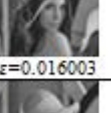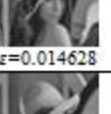
methods p_{max}	Zeroth order approximation direct method	Zeroth order approximation recursive method	Proposed method
10	$\varepsilon=0.083632$	$\varepsilon=0.083632$	$\varepsilon=0.083632$
20	$\varepsilon=0.044057$	$\varepsilon=0.044057$	$\varepsilon=0.044008$
30	$\varepsilon=$ very high	$\varepsilon=0.022432$	$\varepsilon=0.022161$
40		$\varepsilon=0.018796$	$\varepsilon=0.018643$
50		$\varepsilon=0.041729$	$\varepsilon=0.018142$
60		$\varepsilon=0.074614$	$\varepsilon=0.016003$
70		$\varepsilon=0.202217$	$\varepsilon=0.014628$
80		$\varepsilon=0.416709$	$\varepsilon=0.013769$

Fig.6: Reconstructed image of Lena 64×64 **using *PZMs*, with different orders,** $p_{max}=10$ *to* 80 **for outer circle.**

4.2 Rotation Invariance

Rotation invariance is one of the most useful characteristics of *PZMs*. This property is, however, affected by various errors and the discrete nature of the image function. In order to analyze the effects of errors on rotation invariance, all twelve standard images are resized to 64×64 pixels and rotated by angles ranging from 0° to 90° with an interval of 10°. In order to evaluate quantitatively the effect of rotation, we define the average mean square error, *MSE*, of *PZMs* magnitudes as

$$MSE=\frac{1}{L}\sum_{p=0}^{p_{max}}\sum_{q=0}^{p}\left(\left|A_{pq}^{\alpha}\right|-\left|A_{pq}\right|\right)^2 \qquad 18)$$

where $\alpha=0^o,10^o,20^o,...,90^o$ are the angles of rotation set in our experiments, A_{pq} and A_{pq}^{α} are the *PZMs* of the non-rotated and rotated images, respectively, and L is the total number of moments for a given maximum order p_{max}, which is given as $L=(1+p_{max})(2+p_{max})/2$. The average *MSE* is

plotted for various angles of rotation for the twelve standard images for various methods by taking $p_{max}=20$ and the results are shown in Fig.7 and Fig.8 corresponding to inscribed circle and outer circle, respectively. It is observed that the curves for the direct and recursive methods overlap meaning thereby that they reflect the same trend for rotation invariance. The average value of *MSE* is quite high for $p_{max}=20$. On the other hand, the proposed method provides small values of average *MSE* as compared to direct method and recursive method. This shows that the rotation invariance property is severely affected by the presence of these errors.
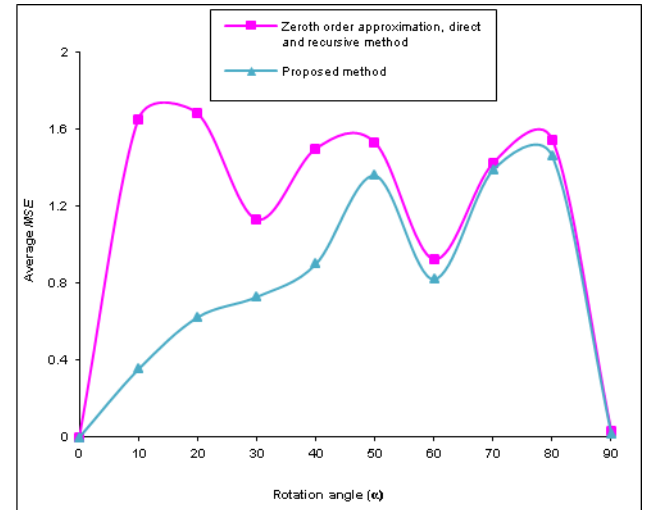

Fig.7: Effect of rotation on average mean square error (*MSE*) of *PZMs* magnitude for $p_{max}=20$ **on 12 standard images (inscribed circle).**
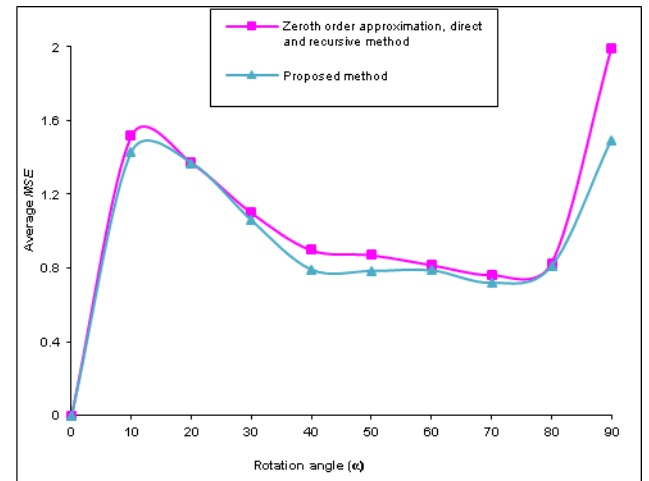

Fig.8: Effect of rotation on average mean square error (*MSE*) of *PZMs* magnitude for $p_{max}=20$ **on 12 standard images (outer circle).**

5. CONCLUSIONS

The computation of *PZMs* suffers from discretization error, geometric error and numerical integration error. The presence of these errors affects the performance of image description capability of these moments. These errors are more pronounced in small images. In this paper, we propose an approach through image interpolation which reduces these

errors. The proposed method uses bi-cubic interpolation of image function which provides higher resolution of image function, thereby, enhancing the number of sampling points. We know that the geometric error and numerical integration error are reduced if more number of sampling points are available for *PZMs* calculation. Thus the proposed method not only reduces discretization error but also reduces geometric error and numerical integration error. The enhanced accuracy is reflected through better image reconstruction and improved invariance to rotation. The proposed method for the computation of *PZMs* does not turn out to be prohibitive because of the computation of kernel functions at more than one location. It requires only 2.97 seconds, 3.47 seconds as compared to the direct method which requires 5.84 seconds, 6.93 seconds, respectively for inscribed circle and outer circle for 64×64 pixels image for $p_{max} = 20$. Thus the method can be used for applications such as optical character recognition and template matching where small images are used.

6. REFERENCES

[1] Hu, M.K. 1962. Visual pattern recognition by moment invariants, IRE Trans. Inf. Theory vol 8, 179–187.

[2] Papakostas, G.A., Boutalis, Y.S., Karras, D.A., Mertzios, B.G. 2010. Efficient computation of Zernike and pseudo Zernike moments for Pattern Classification Applications, Pattern recog. and image analysis, vol 20, no 1, 56-64.

[3] Wang, X-Y, Yu, Y-J, Yang, H.Y. 2011. An effective image retrieval scheme using color, texture and shape features, Computer Standards and Interfaces, vol 33, 59-68.

[4] Alt, F.L. 1962. Digital pattern recognition by moments, Journal of ACM, vol 9, no 2, 240–258.

[5] Xin, Y., Liao, S., Pawlak, M. 2004. Geometrically robust image watermark via pseudo Zernike moments, in proc. of 2004 Canadian Conf. on Electrical and Comp. Engg., vol 2, 939-942.

[6] Pang, Y-H, Teoh, A.B.J., Ngo, D.C.L. 2006. A discriminate pseudo Zernike moments in face recognition, J. Res. Pract. Inf. Technol. vol 38, no. 2, 197–211.

[7] Wallin, A., Kubler, O. 1995. Complete sets of complex Zernike moment invariants and the role of the pseudo invariants, IEEE Trans. Pattern. Anal. Mach. Intell, vol 17, 1106-1110.

[8] Zhang, D. Lu, G. 2004. View of shape representation and description techniques, Pattern Recognition, vol 37, 1–19.

[9] Li, B., Zhang, G., Fu, B. 2010. Accurate compuation and error analysis of pseudo Zernike Moments, 2nd International Confrence on Education Technology and Computer (ICETC), Shanghai, China.

[10] Teh, C.H., Chin, R.T. 1988. On image analysis by the methods of moments, IEEE Trans. Pat. Anal. Mach. Intell., vol 10, no 4, 496-513.

[11] Chong, C.W., Raveendran, P., Mukundan, R. 2003. The scale invariants of pseudo Zernike moments, Pattern anal applic, vol 6, 176-184.

[12] Singh, C. Improved quality of reconstructed images using floating point arithmetic for moment calculation, Pattern Recognition, vol 39, 2047–2064.

[13] Liao, S.X., Pawlak, M. 1998. On the accuracy of Zernike moments for image analysis, IEEE Trans. Pattern Anal. Mach. Intell., vol 20, no12, 1358-1364.

[14] Wee, C.Y., Paramesran, R. 2007. On the computational aspects of Zernike moments, Image and Vision Computing, vol 25, 967-980.

[15] Al-Rawi, M.S. 2007. Fast computation of pseudo-Zernike moments, J. Real Time Image Processing, vol 5,no 1, 3-10.

[16] Keys, R. G. 1981. Cubic convolution interpolation for digital image processing, IEEE Trans. Acoust., Speech and Signal Process., vol 29, no 2, 1153–1160.

[17] Reichenbach, S.E., Geng, F. 2003. Two-dimensional cubic convolution, IEEE Trans. Image Process., vol 12, no 8, 857–865.